HHS Public Access

Author manuscript

Toxicol Appl Pharmacol. Author manuscript; available in PMC 2015 May 01.

Published in final edited form as:

Toxicol Appl Pharmacol. 2014 May 1; 276(3): 165–170. doi:10.1016/j.taap.2014.02.005.

Reactive oxygen species contribute to arsenic-induced EZH2 phosphorylation in human bronchial epithelial cells and lung cancer cells

Lingzhi Li, **Ping Qiu**, **Bailing Chen**, **Yongju Lu**, **Kai Wu**, **Chitra Thakur**, **Qingshan Chang**, **Jiaying Sun**, and **Fei Chen**[*]

Department of Pharmaceutical Sciences, Eugene Applebaum College of Pharmacy and Health Sciences, Wayne State University, 259 Mack Avenue, Detroit, MI 48201, USA

Abstract

Our previous studies suggested that arsenic is able to induce serine 21 phosphorylation of the EZH2 protein through activation of JNK, STAT3, and Akt signaling pathways in the bronchial epithelial cell line, BEAS-2B. In the present report, we further demonstrated that reactive oxygen species (ROS) were involved in the arsenic-induced protein kinase activation that leads to EZH2 phosphorylation. Several lines of evidence supported this notion. First, the pretreatment of the cells with *N*-acetyl-L-cysteine (NAC), a potent antioxidant, abolishes arsenic-induced EZH2 phosphorylation along with the inhibition of JNK, STAT3, and Akt. Second, H_2O_2, the most important form of ROS in the cells in response to extracellular stress signals, can induce phosphorylation of the EZH2 protein and the activation of JNK, STAT3, and Akt. By ectopic expression of the myc-tagged EZH2, we additionally identified direct interaction and phosphorylation of the EZH2 protein by Akt in response to arsenic and H_2O_2. Furthermore, both arsenic and H_2O_2 were able to induce the translocation of ectopically expressed or endogenous EZH2 from nucleus to cytoplasm. In summary, the data presented in this report indicate that oxidative stress due to ROS generation plays an important role in the arsenic-induced EZH2 phosphorylation.

Keywords

Arsenic; Oxidative stress; EZH2; Akt; Phosphorylation; Cytoplasmic translocation

Introduction

Arsenic is an environmental and carcinogenic metalloid found in water, earth crust, food, plants, and some other natural depositions (Nordstrom, 2002). Certain industrial settings can also release arsenic into the environment through the industry activities, such as mining, mineral refining, pesticide manufacturing, and wood preservation (Garelick et al., 2008). In general, the organic form of arsenic that is compounded with carbon and found in certain

[*]Corresponding author at: Department of Pharmaceutical Sciences, Wayne State University, 259 Mack Avenue, Detroit, MI 48291, USA. fchen@wayne.edu (F. Chen).

seafood or plant, is considered as less toxic. In contrast, the inorganic form of arsenic that is compounded with sulfur and chloride and, among others, is highly toxic. The International Agency for Research on Cancer (IARC) classifies inorganic arsenic and its compounds as group I carcinogens (IARC, 1987). Well-documented evidence showed that chronic exposure to arsenic increased the risks of cancer development, including cancers in lung, skin, bladder, kidney, and liver (Ren et al., 2011). Currently, more than 137 million people are exposed to arsenic in ground water worldwide.

A number of reports revealed that inorganic arsenic, especially the trivalent arsenic (As^{3+}), may induce excessive generation of the reactive oxygen species (ROS) in mammalian cells (Chou et al., 2004; Hei et al., 1998; Wang et al., 2013; Zhang et al., 2011). ROS were able to cause genetic mutation and cancer through the mechanism of DNA damage, activation of the oncogenic kinases (Wang et al., 2012), or oxidation of the important lipids and proteins to inactivate DNA repairing machineries, such as poly(ADP ribose) polymerase (PARP)-1 (Hubaux et al., 2012; Wang et al., 2013). There are several cellular sources of ROS induced by As^{3+}. First, As^{3+} can induce the release of redox active iron from ferritin to catalyzes the Haber–Weiss Fenton reaction, leading to the generation of the hydroxyl radical (Ahmad et al., 2000). Second, As^{3+} has been viewed as a potent activator of the NADPH oxidase that is bound to the cell membrane for the release of superoxide anion (Chou et al., 2004). Third, As^{3+} may alter the membrane potential of the mitochondria and the subsequent increased generation of ROS from mitochondria (Woo et al., 2002). Lastly, the metabolism of As^{3+} to pentavalent arsenic involves the reduction of H_2O, which generates H_2O_2, and some metabolic intermediates, such as dimethylarsine peroxyl radical [$(CH_3)_2AsOO•$] (Valko et al., 2006; Yamanaka et al., 2001).

Enhancer of Zeste homolog 2 (EZH2) is an enzymatic subunit of the PRC2 complex responsible for the tri-methylation of lysine 27 on histone H3 (H3K27me3) (Hock, 2012). Emerging evidence suggested that many types of cancers exhibited increased expression or activity of EZH2 that represses the expression of tumor suppressors and tumor-suppressive microRNAs, such as, ARF, p57KIP2, FBXO32, p27, BRCA1, and miR-29 (Zhang et al., 2012). In our previous study, we have discovered that As^{3+} is capable of inducing serine 21 phosphorylation of the EZH2 protein (pEZH2) and provided evidence indicating the importance of the upstream protein kinase pathways in this bioprocess (Chen et al., 2013). The present study is to delineate whether ROS are the key mediators for As^{3+}-induced pEZH2 phosphorylation.

Materials and methods

Cell lines and reagents

The human bronchial epithelial cell line BEAS-2B was obtained from the American Type Culture Collection (ATCC, Manassas, VA). The cells were cultured in Dulbecco's modified Eagle's medium (DMEM, Invitrogen, Grand Island, NY) containing 5% fetal bovine serum (FBS, Invitrogen), 1% penicillin, and 1%L-glutamine (Sigma) at 37 °C humidified incubator with 5% CO_2. The human embryonic kidney 293 cell line was purchased from ATCC and maintained in DMEM containing 10% FBS, 1% penicillin, and 1% L-glutamine at 37 °C humidified incubator with 5% CO_2. The non-small cell lung cancer cell line A549 was from

ATCC and cultured in RPMI-1640 medium supplemented with 10% FBS, 1% penicillin, and 1% ι-glutamine (Sigma). The cells were seeded in 6-well plates. When the cells reached 70%–80% confluency, hydrogen peroxide (Sigma), As^{3+}, or NAC (*N*-acetyl-L-cysteine, Sigma) were added for the indicated concentrations and times.

Plasmid preparation and transfection

pGFP-EZH2-WTand p3myc-EZH2-WT are gifts from Dr. Mien-Chie Hung (Department of Molecular and Cellular Oncology, University of Texas). The plasmid DNA was amplified from DH5α competent cells (Invitrogen) and purified using Plasmid Purification Kit (QIAGEN) according to the manufacturer's protocol. BEAS-2B or HEK-293 cells in 6-well plates were transfected with 2 μg plasmic DNA using Lipofectamine 2000 Transfection Reagent (Invitrogen) or Nucleofector (Lonza) with program T020. The cells were then cultured for 24 h followed by the treatment of the cells with As^{3+} or H_2O_2 for the indicated times.

Cellular fractionation and Western blotting

For nuclear and cytoplasmic fractionations, a NE-PER nuclear and cytoplasmic fractionation kit (Thermo Scientific, Rockford IL) was used according to the manufacturer's protocol. Fractions were then analyzed by regular Western blotting using GAPDH and lamin A/C as cytoplamic and nuclear reference, respectively. For regular Western blotting, the cell lysates were prepared by RIPA cell lysis buffer (Cell Signalling) followed by ultrasonication and centrifugation. The supernatants were aspirated and proteins were quantified using a SpectraMax spectrophotometer (MDA Analytical Technologies). LDS sample buffer (Invitrogen) and dithiothreitol were added before denature. The samples were separated on 7.5% or 10% SDS–PAGE running gel and then transferred to methanol wetted PVDF membranes. The membranes were blocked in 5% non-fat milk in TBST and incubated with the indicated primary antibodies at 4 °C overnight and then incubated with second antibodies at room temperature for 1 hour and washed with TBST 3 times for 10 min each. The protein levels were detected using CDP-Star Reagent (New England Biolabs). The primary antibodies used in Western blotting include anti-phopho-EZH2 (Ser21) (Abcam), anti-phospho-JNK (Cell Signaling), anti-phospho-Akt(Ser473) (Cell Signaling), anti-phospho-Stat3(Ser 727) (Cell Signaling), anti-phospho-p38 (Cell Signaling), anti-phopho-ERK (Cell Signaling), anti-EZH2 (Cell Signaling), anti- JNK (Cell Signaling), anti-Stat3 (Cell Signaling), anti-p38 (Cell Signaling), anti-ERK (Cell Signaling), anti-GFP (Santa Cruz), anti-phospho-Akt substrate RXRXXS*/T* (Cell Signaling), anti-GAPDH (Cell Signaling), and anti-β-actin (Sigma).

Immunoprecipitation (IP) and fluorescent microscopy

After the indicated treatments, the cells were collected in IP lysis buffer and fragmented through passing the cells in a syringe equipped with 21.5 needle for 10–15 times and then incubating with the specific antibodies or IgG that were conjugated with agarose beads at 4 °C agitation overnight. For fluorescent microscopy, the cells were fixed by 4% paraformaldehyde at room temperature for 15 min. DNA was stained with 1 μg/ml of DAPI.

Statistics

Microsoft Excel was used for statistical analyses of the quantitative data. The data are expressed as the mean ± standard deviation (SD), and Student's *t*-tests were used to determine the statistical significance of differences between samples treated under different conditions. Differences were considered statistically significant when $*p < 0.05$ or $**p < 0.01$.

Result

As^{3+}-induced EZH2 phosphorylation is ROS dependent in BEAS-2B cells

In agreement with our previous report, we observed that As^{3+} is able to induce serine 21 (S21) phosphorylation of the EZH2 in human bronchial epithelial cell line, BESA-2B cells (Fig. 1A). To determine the involvement of oxidative stress resulted from ROS generation in this As^{3+}-induced EZH2 phosphorylation, we pre-treated the cells with 20 mM *N*-acetyl-L-cysteine (NAC), a general antioxidant that provides the cells with sufficient amount of glutathione to minimize the oxidation of cellular proteins, lipids, and DNA (Sadowska et al., 2006), for 2 h and then treated the cells with 20 μM As^{3+} for 1,2, or 4 h. A significant reduction in EZH2 phosphorylation was noted in the cells treated with NAC (Fig. 1A). NAC is also capable of inhibiting As^{3+}-induced activation of Akt, STAT3, and JNK (Fig. 2B and C), the upstream kinases associated with the S21 phosphorylation of the EZH2. In addition, NAC is also potent in diminishing the As^{3+}-induced activation of ERK and p38 (Fig. 1D), two mitogen-activated protein kinases that respond to the oxidative stress. To validate the contribution of ROS in As^{3+}-induced S21 phosphorylation of the EZH2, we also tested the capability of H_2O_2, one of the most abundant and important ROS, on EZH2 phosphorylation and kinase activation. Indeed, an earlier occurrence of S21 phosphorylation of the EZH2was noted in the cells treated with 0.2 m MH_2O_2 for 5 to 15 min (Fig. 1E), which correlates with the time-dependent activation of Akt and the dose-dependent Akt activation in the cells treated with different concentrations of H_2O_2 for 5 min (Figs. 1E and 1F).

ROS contribute to As^{3+}-induced EZH2 phosphorylation in A549 cells

To explore whether the above observations are cell type specific or not, we extended this study in other type of cells too. A549 is a cell line derived from the non-small cell lung cancer (NSCLC) with some features of alveolar type II cells. The S21 phosphorylation of the EZH2 could be observed in the A549 cells treated with 20 μM As^{3+} for 1 to 4 h with a peak phosphorylation at 2 h, which is roughly parallel with the pattern of Akt activation by As^{3+} (Fig. 2A). A significant decrease of both EZH2 phosphorylation and Akt activation in response to As^{3+} was noted in the cells pre-treated with 10 or 20 mM NAC (Fig. 1A), indicating that oxidative stress due to ROS induction by As^{3+} is also involved in the S21 phosphorylation of the EZH2 protein in A549 cells. To address this notion further, the A549 cells were treated with different concentrations of H_2O_2 for 5 min or 500 μMH_2O_2 for 5 to 60 min. As depicted in Fig. 2B, H_2O_2 is able to induce S21 phosphorylation of the EZH2 along with the activation of the upstream kinases, including JNK, STAT3, and Akt.

To extend above observations, we also tested the inducibility of EZH2 phosphorylation by As^{3+} at much lower concentrations from 0.25 to 4 μM in the cells cultured for a prolonged

time, 72 h. We noted that lower concentrations of As^{3+} was able to induce JNK and p38 activation in a clear dose-dependent manner (Fig. 2C and data not shown). However, a significant Akt activation by lower concentrations of As^{3+} could not be detected (top two panels, Fig. 2C). The treatment of the cells with 0.25 or 2 μM As^{3+}-induced S21 phosphorylation of EZH2 (Fig. 2D). Unexpectedly, NAC appeared to be unable to inhibit the EZH2 phosphorylation induced by As^{3+} at lower concentrations. In other experiments, we demonstrated that prolonged incubation of the cells with NAC, e.g., 72 h, enhanced both basal and As^{3+}-induced p38 activation, possibly because of stress responses due to the overwhelmed reduction condition. Accordingly, we speculate that different mechanisms may be involved in the EZH2 phosphorylation induced by low and high concentrations of As^{3+}, respectively.

Both As^{3+} and H_2O_2 induce exogenous EZH2 phosphorylation through the direct interaction of Akt and EZH2

As an arginine (Arg, R)-directed or AGC-family kinase, Akt can directly phosphorylate serine (Ser)/Threonine (Thr) in a conserved motif, RXRXXS/T, characterized by R at positons – 5 and – 3 (Alessi et al., 1996). Accordingly, proteins containing RXRXXS/T motif can be phosphorylated by Akt, which can be recognized by anti-RXRXXS*/T* motif antibody (anti-Akt substrate antibody, "*" indicates phosphorylation). The human EZH2 protein contains RKRVKS21 motif that is in consensus with the conserved Akt phosphorylation site. To determine if As^{3+} can induce S21 phosphorylation of the exogenous EZH2 by Akt, the HEK-293 cells were transfected with a 3myc-tagged EZH2 followed by As^{3+} treatment. In the Western blotting results as shown in Fig. 3A, the anti-Akt substrate antibody detected several bands with molecular weights around 170, 130, 95, 72, and 50 kDa (Fig. 3A, pointed by small triangles) in the cells treated with As^{3+}. Re-probing of the membrane with antibodies against myc-tag and EZH2 suggested that the band at position 95 kDa contains both the endogenous and the exogenously transfected EZH2 proteins that were phosphorylated by Akt. It remains to be determined about the nature of other bands at the positions 170, 130, 72, and 50 kDa that are phosphorylated by Akt as indicated by the anti-pAkt substrate antibody. The intensity of these bands was significantly decreased in the cells treated with NAC, suggesting that ROS play important role in As^{3+}-induced phosphorylation of these proteins by Akt. To further validate the involvement of ROS in the phosphorylation of these proteins, the transfected HEK-293 cells were treated with 0.5 mM H_2O_2 for 5 to 30 min and then the cells were subjected to Western blotting using the anti-pAkt substrate antibody. A similar pattern of band detecting was noted in the cells treated with As^{3+} and H_2O_2 (comparing lane 2 with lanes 3–5, Fig. 3B).

To determine whether As^{3+}-induced EZH2 S21 phosphorylation is through direct interaction of Akt and EZH2 in the HEK-293 cells transfected with myc-tagged EZH2, an immunoprecipitation (IP) was performed to pull down the myc-tagged exogenous EZH2. As shown in Fig. 3C, the anti-pAkt substrate antibody recognized the phosphorylated form of myc-tagged EZH2 that was precipitated from the As^{3+}-treated cells. The pretreatment of the transfected cells with NAC diminished As^{3+}-induced phosphorylation of the exogenous EZH2 protein. Again, H_2O_2 was able to induce this Akt-dependent phosphorylation of the exogenous EZH2. Furthermore, when the precipitates from Myc-tag IP were subjected to

Western blotting using antibodies against pAkt and Akt, respectively, a predominant pAktS473 signal was detected in the IP from As^{3+}- or H_2O_2-treated cells (Fig. 3C), indicating the direct interaction of the activated Akt with the myc-tagged EZH2 in the cells in response to As^{3+} and H_2O_2. The interaction of the non-activated Akt with the myc-tagged EZH2 was negligible.

Involvement of ROS in As^{3+}-induced cytoplasmic translocation of the EZH2 protein

In BEAS-2B cells, we had previously shown the cytoplasmic translocation of the S21-phosphorylated endogenous EZH2 from nuclei in response to As^{3+} treatment (Chen et al., 2013). To investigate if As^{3+} is able to induce the same translocation of the exogenous EZH2, the BEAS-2B cells expressing GFP-EZH2 were treated with 20 μM As^{3+} for 2 h. The GFP-EZH2 is exclusively localized in the nuclei of the cells without As^{3+} treatment (Fig. 4A, upper panels). Following As^{3+} treatment, both cytoplasmic and nuclear locations of the GFP-EZH2 were observed (Fig. 4A, bottom panels). Furthermore, As^{3+} appeared to be able to induce the clustering of GFP-EZH2 proteins. These clusters were randomly distributed in both cytoplasm and nucleus. To explore whether oxidative stress is involved in As^{3+}-induced re-distribution of the GFP-EZH2, NAC was applied prior to As^{3+} treatment. As shown in Fig. 4B, NAC prevented the cytoplasmic localization of the GFP-EZH2 induced by either 20 μM or 80 μM As^{3+}, indicating that the oxidative stress is involved in As^{3+}-induced cytoplasmic localization of the EZH2 protein. However, NAC was unable to prevent the nuclear clustering of the exogenous GFP-EZH2 proteins induced by As^{3+}. The possible role of oxidative stress on the intracellular distribution of the EZH2 protein was confirmed by the treatment of the cells with 0.2 mM H_2O_2 that clearly induced cytoplasmic localization of the GFP-EZH2 proteins (Fig. 4B, bottom panels). Semi-quantification suggested a more than 50% inhibition of the As^{3+}-induced cytoplasmic localization of the exogenous EZH2 (GFP-EZH2) by NAC (Fig. 4C).

To additionally confirm the effect of As^{3+} and/or oxidative stress on the cytoplasmic localization of the EZH2 proteins, we fractionated the cell lysates by isolating cytoplasmic and nuclear fractions, respectively, followed by measuring the levels of S21-phosphorylated and the total endogenous EZH2 proteins in response to As^{3+} or H_2O_2 treatment. Although As^{3+} appeared to be unable to affect the nuclear levels of the phosphorylated EZH2 (pEZH2) and EZH2, As^{3+} was able to increase both pEZH2 and EZH2 in the cytoplasmic fraction (Fig. 5A). The pretreatment of the cells with 20 mM NAC reduced As^{3+}-induced pEZH2 in the cytoplasmic fraction significantly. NAC was also able to reduce the level of total EZH2 in the cytoplasmic fraction, although with a lesser extent relative to its effect on the phosphorylated EZH2.

H_2O_2 could transiently induce the increase of both phosphorylated and total EZH2 in the cytoplasm (Fig. 5B). However, this effect of H_2O_2 was rapidly diminished after 10 min of H_2O_2 treatment, possibly due to the fast elimination of H_2O_2 by the medium, the cellular peroxisomes that contain catalase and the cytoplasmic glutathione peroxidase (GPx) and NADPH (Makino et al., 2004).

Discussion

In the present report, we provide evidence showing that the oxidative stress due to ROS generation contributes to As^{3+}-induced kinase activation that leads to S21 phosphorylation of the EZH2 protein. In addition, oxidative stress is also involved in the direct interaction of the activated Akt and EZH2. Furthermore, oxidative stress appears to be able to induce cytoplasmic localization of the phosphorylated and the non-phosphorylated EZH2 protein in the cells treated with As^{3+}. The pretreatment of the cells with NAC prevented EZH2 phosphorylation and cytoplasmic localization induced by As^{3+}.

EZH2 along with EED, SUZ12, and RbAp46/48 proteins forms polycomb repressive complex 2 (PRC2) that catalyzes the trimethylation of lysine 27 of histone H3 (H3K27me3), a mark of transcriptionally silent or poised chromatin (Margueron and Reinberg, 2011). In the past few years, EZH2 had been the focus of a significant number of biochemical and molecular studies in cancer cells and cancer stem cells. Many independent studies revealed that EZH2 is overexpressed in several common cancers and that the degree of EZH2 overexpression is associated with the aggressiveness of these tumors (Hock, 2012). Such an overexpression of EZH2 was viewed as a major causative force, rather than a result, of the cancer development. Some genetic studies suggested that missense mutation in the catalytic domain causes hyperactivation of the EZH2 protein and increased incidents of malignancies, such as neuroblastoma and lymphoma (Crea, 2012). Additional evidence also indicated that the overactivation of EZH2 is responsible for the increased aggressiveness of the breast cancer associated with the loss of BRCA1 tumor suppressor (Wang and Huang, 2013). In human prostate cancer, EZH2 is one of the most important oncogenic factors for the initiation and progression of the tumor, as revealed by the fact that the inactivation of EZH2 by chemical inhibitor DZNep reduced tumor size and invasion significantly (Deb et al., 2013). A well-accepted and simplified explanation for the oncogenic role of EZH2 is that EZH2 inhibits the expression of tumor suppressor genes and DNA repair genes through the PRC2-dependent establishment of the silent chromatin that enriched with H3K27me3. A most recent study, however, suggested a PRC2-independent role of EZH2 in glioblastoma stem cells (GSC) (Kim et al., 2013). Following Akt-mediated S21 phosphorylation, EZH2 can directly bind to and induces methylation of lysine 180 (K180) of the STAT3 protein, leading to a sustained activation of the transcriptional activity of the STAT3 and the maintenance of the stemness of the GSC (Kim et al., 2013).

S21 phosphorylation of EZH2 by Akt kinase has been first demonstrated in breast cancer cells treated with insulin-like growth factor I (IGF-I) or estrogen (Bredfeldt et al., 2010; Cha et al., 2005). In BEAS-2B cells, we had also noticed S21 phosphorylation of the EZH2 protein through the activation of the JNK-STAT3-Akt signaling axis in response to As^{3+} (Chen et al., 2013). The present report further unraveled the importance of oxidative stress or ROS in this As^{3+}-induced EZH2 phosphorylation, which confirmed our previous findings showing that As^{3+} is able to induce ROS generation in the non-transformed BEAS-2B cells (Chang et al., 2010). Given the critical roles of ROS and EZH2 in human cancers related to environmental exposure, the data from this report may shed new light on the prevention or treatment of human lung cancer or other cancers resulting from environmental exposure to As^{3+} or other carcinogens.

Acknowledgment

We thank Dr. Mien-Chie Hung from the Department of Molecular and Cellular Oncology, University of Texas, for providing pGFP-EZH2-WT and p3myc-EZH2-WT expression vectors. This work was supported by NIH grant nos. R01 ES017217 and R01 ES020137 to FC.

References

Ahmad S, Kitchin KT, Cullen WR. Arsenic species that cause release of iron from ferritin and generation of activated oxygen. Arch. Biochem. Biophys. 2000; 382:195–202. [PubMed: 11068869]

Alessi DR, Caudwell FB, Andjelkovic M, Hemmings BA, Cohen P. Molecular basis for the substrate specificity of protein kinase B; comparison with MAPKAP kinase-1 and p70 S6 kinase. FEBS Lett. 1996; 399:333–338. [PubMed: 8985174]

Bredfeldt TG, Greathouse KL, Safe SH, Hung MC, Bedford MT, Walker CL. Xenoestrogen-induced regulation of EZH2 and histone methylation via estrogen receptor signaling to PI3K/AKT. Mol. Endocrinol. 2010; 24:993–1006. [PubMed: 20351197]

Cha TL, Zhou BP, Xia W, Wu Y, Yang CC, Chen CT, Ping B, Otte AP, Hung MC. Akt-mediated phosphorylation of EZH2 suppresses methylation of lysine 27 in histone H3. Science. 2005; 310:306–310. [PubMed: 16224021]

Chang Q, Pan J, Wang X, Zhang Z, Chen F, Shi X. Reduced reactive oxygen species-generating capacity contributes to the enhanced cell growth of arsenic-transformed epithelial cells. Cancer Res. 2010; 70:5127–5135. [PubMed: 20516118]

Chen B, Liu J, Chang Q, Beezhold K, Lu Y, Chen F. JNK and STAT3 signaling pathways converge on Akt-mediated phosphorylation of EZH2 in bronchial epithelial cells induced by arsenic. Cell Cycle. 2013; 12:112–121. [PubMed: 23255093]

Chou WC, Jie C, Kenedy AA, Jones RJ, Trush MA, Dang CV. Role of NADPH oxidase in arsenic-induced reactive oxygen species formation and cytotoxicity in myeloid leukemia cells. Proc. Natl. Acad. Sci. U. S. A. 2004; 101:4578–4583. [PubMed: 15070760]

Crea F. Histone code, human growth and cancer. Oncotarget. 2012; 3:1–2. [PubMed: 22287500]

Deb G, Thakur VS, Gupta S. Multifaceted role of EZH2 in breast and prostate tumorigenesis: epigenetics and beyond. Epigenetics. 2013; 8:464–476. [PubMed: 23644490]

Garelick H, Jones H, Dybowska A, Valsami-Jones E. Arsenic pollution sources. Rev. Environ. Contam. Toxicol. 2008; 197:17–60. [PubMed: 18982996]

Hei TK, Liu SX, Waldren C. Mutagenicity of arsenic in mammalian cells: role of reactive oxygen species. Proc. Natl. Acad. Sci. U. S. A. 1998; 95:8103–8107. [PubMed: 9653147]

Hock H. A complex polycomb issue: the two faces of EZH2 in cancer. Genes Dev. 2012; 26:751–755. [PubMed: 22508723]

Hubaux R, Becker-Santos DD, Enfield KS, Lam S, Lam WL, Martinez VD. Arsenic, asbestos and radon: emerging players in lung tumorigenesis. Environ. Health. 2012; 11:89. [PubMed: 23173984]

IARC. Overall evaluations of carcinogenicity: an updating of IARC Monographs volumes 1 to 42. IARC Monogr Eval Carcinog Risks Hum. 1987; (Suppl 7):1–440. (PMID: 3482203).

Kim E, Kim M, Woo DH, Shin Y, Shin J, Chang N, Oh YT, Kim H, Rheey J, Nakano I, et al. Phosphorylation of EZH2 activates STAT3 signaling via STAT3 methylation and promotes tumorigenicity of glioblastoma stem-like cells. Cancer Cell. 2013; 23:839–852. [PubMed: 23684459]

Makino N, Sasaki K, Hashida K, Sakakura Y. A metabolic model describing the H2O2 elimination by mammalian cells including H2O2 permeation through cytoplasmic and peroxisomal membranes: comparison with experimental data. Biochim. Biophys. Acta. 2004; 1673:149–159.

Margueron R, Reinberg D. The polycomb complex PRC2 and its mark in life. Nature. 2011; 469:343–349. [PubMed: 21248841]

Nordstrom DK. Public health. Worldwide occurrences of arsenic in ground water. Science. 2002; 296:2143–2145. [PubMed: 12077387]

Ren X, McHale CM, Skibola CF, Smith AH, Smith MT, Zhang L. An emerging role for epigenetic dysregulation in arsenic toxicity and carcinogenesis. Environ. Health Perspect. 2011; 119:11–19. [PubMed: 20682481]

Sadowska AM, Verbraecken J, Darquennes K, De Backer WA. Role of *N*-acetylcysteine in the management of COPD. Int. J. Chron. Obstruct Pulm. Dis. 2006; 1:425–434.

Valko M, Rhodes CJ, Moncol J, Izakovic M, Mazur M. Free radicals, metals and antioxidants in oxidative stress-induced cancer. Chem. Biol. Interact. 2006; 160:1–40. [PubMed: 16430879]

Wang L, Huang H. EZH2 takes the stage when BRCA1 loses. Cell Cycle. 2013; 12:3575–3576. [PubMed: 24121664]

Wang X, Mandal AK, Saito H, Pulliam JF, Lee EY, Ke ZJ, Lu J, Ding S, Li L, Shelton BJ, et al. Arsenic and chromium in drinking water promote tumorigenesis in a mouse colitis-associated colorectal cancer model and the potential mechanism is ROS-mediated Wnt/beta-catenin signaling pathway. Toxicol. Appl. Pharmacol. 2012; 262:11–21. [PubMed: 22552367]

Wang F, Zhou X, Liu W, Sun X, Chen C, Hudson LG, Jian Liu K. Arsenite-induced ROS/RNS generation causes zinc loss and inhibits the activity of poly(ADP-ribose) polymerase-1. Free Radic. Biol. Med. 2013; 61C:249–256. [PubMed: 23602911]

Woo SH, Park IC, Park MJ, Lee HC, Lee SJ, Chun YJ, Lee SH, Hong SI, Rhee CH. Arsenic trioxide induces apoptosis through a reactive oxygen species-dependent pathway and loss of mitochondrial membrane potential in HeLa cells. Int. J. Oncol. 2002; 21:57–63. [PubMed: 12063550]

Yamanaka K, Takabayashi F, Mizoi M, An Y, Hasegawa A, Okada S. Oral exposure of dimethylarsinic acid, a main metabolite of inorganic arsenics, in mice leads to an increase in 8-Oxo-2'-deoxyguanosine level, specifically in the target organs for arsenic carcinogenesis. Biochem. Biophys. Res. Commun. 2001; 287:66–70. [PubMed: 11549254]

Zhang Z, Wang X, Cheng S, Sun L, Son YO, Yao H, Li W, Budhraja A, Li L, Shelton BJ, et al. Reactive oxygen species mediate arsenic induced cell transformation and tumorigenesis through Wnt/beta-catenin pathway in human colorectal adenocarcinoma DLD1 cells. Toxicol. Appl. Pharmacol. 2011; 256:114–121. [PubMed: 21854796]

Zhang X, Zhao X, Fiskus W, Lin J, Lwin T, Rao R, Zhang Y, Chan JC, Fu K, Marquez VE, et al. Coordinated silencing of MYC-mediated miR-29 by HDAC3 and EZH2 as a therapeutic target of histone modification in aggressive B-cell lymphomas. Cancer Cell. 2012; 22:506–523. [PubMed: 23079660]

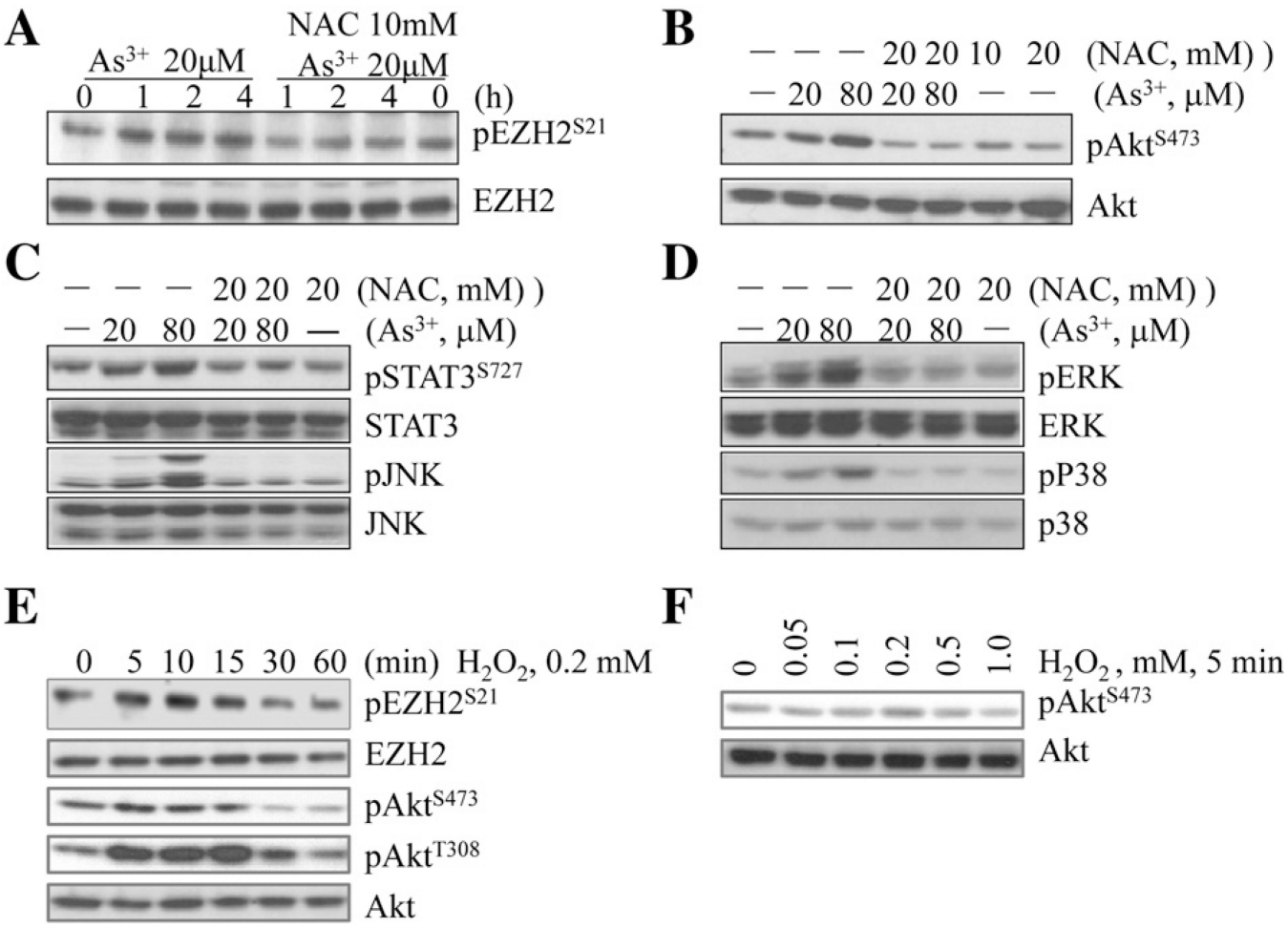

Fig. 1.

Involvement of oxidative stress in As^{3+}-induced kinase activation and EZH2 phosphorylation in BEAS-2B cells. (A) BEAS-2B cells were treated with 20 μM As^{3+} for 0, 1, 2, or 4 h with or without NAC pretreatment for 2 h. S21 phosphorylation of the EZH2 ($pEZH2^{S21}$) protein was determined by Western blotting. The most right lanes (0 h As^{3+}) are NAC only treatment. (B–D) The activation of Akt (B), STAT3 and JNK (C), and Erk and p38 (D) were determined in the BEAS-2B cells treated with 20 or 80 μM As^{3+} for 2 h in the presence or absence of NAC pretreatment for 2 h. In each panel, the most right lanes (without As^{3+}, —) are NAC only groups. (E) H_2O_2 induces $pEZH2^{S21}$ and Akt activation in a time-dependent manner. (F) Dose-dependent activation of Akt kinase in the BEAS-2B cells treated with the indicated concentrations of H_2O_2 for 5 min.

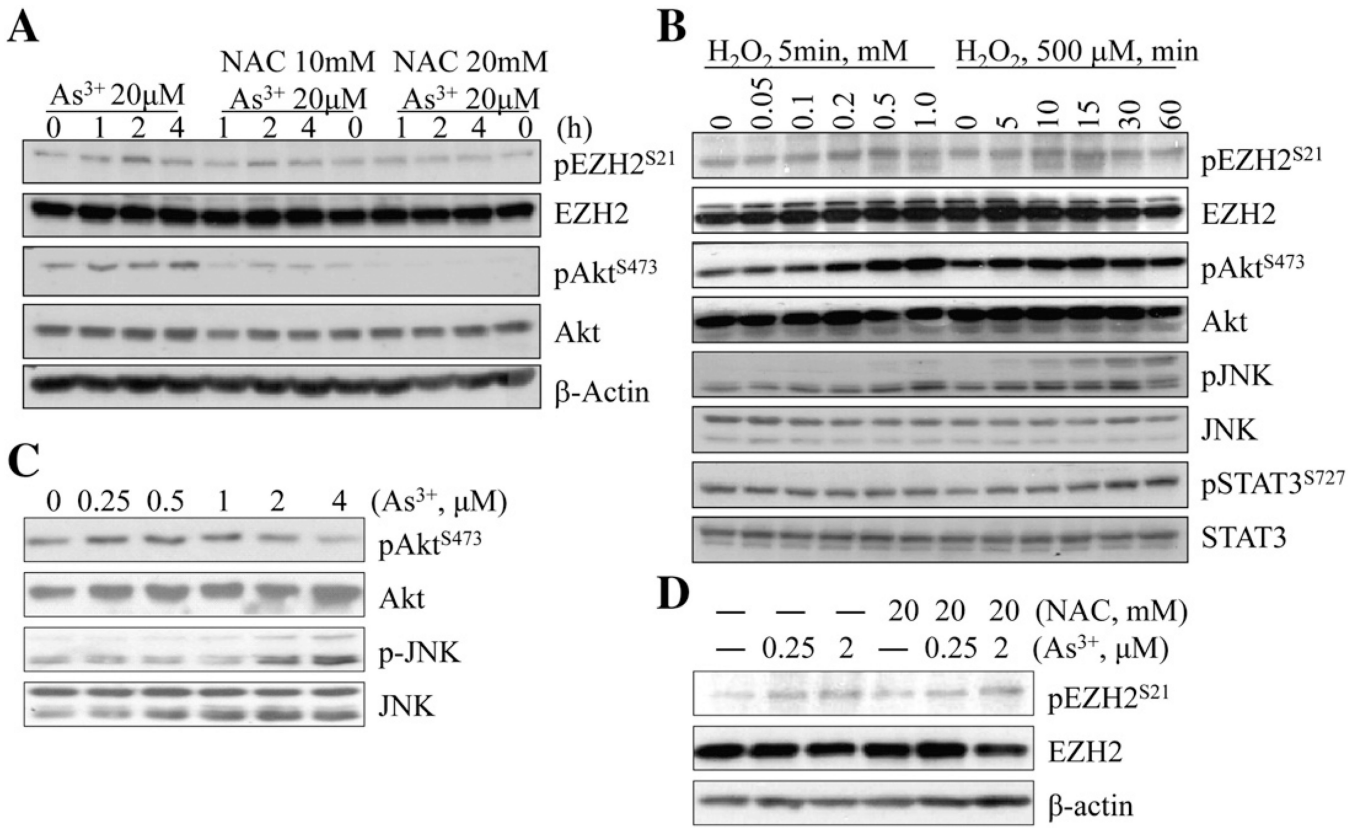

Fig. 2.

Oxidative stress contributes to As^{3+}-induced EZH2 phosphorylation and kinase activation in A549 cells. (A) A549 cells were treated with 20 μM As^{3+} for the indicated time with or without NAC pretreatment for 2 h. The levels of $pEZH2^{S21}$ and Akt activation were determined by Western blotting. The NAC only groups were indicated as 0 h As^{3+} treatment. (B) Dose- and time-dependent EZH2 phosphorylation and kinases activation in A549 cells treated with H_2O_2. (C) Lower concentrations of As^{3+} induce JNK but not Akt activation in the A549 cells treated with As^{3+} for 72 h. (D) NAC was unable to inhibit lower concentration As^{3+}-induced EZH2 phosphorylation in the cells cultured for 72 h.

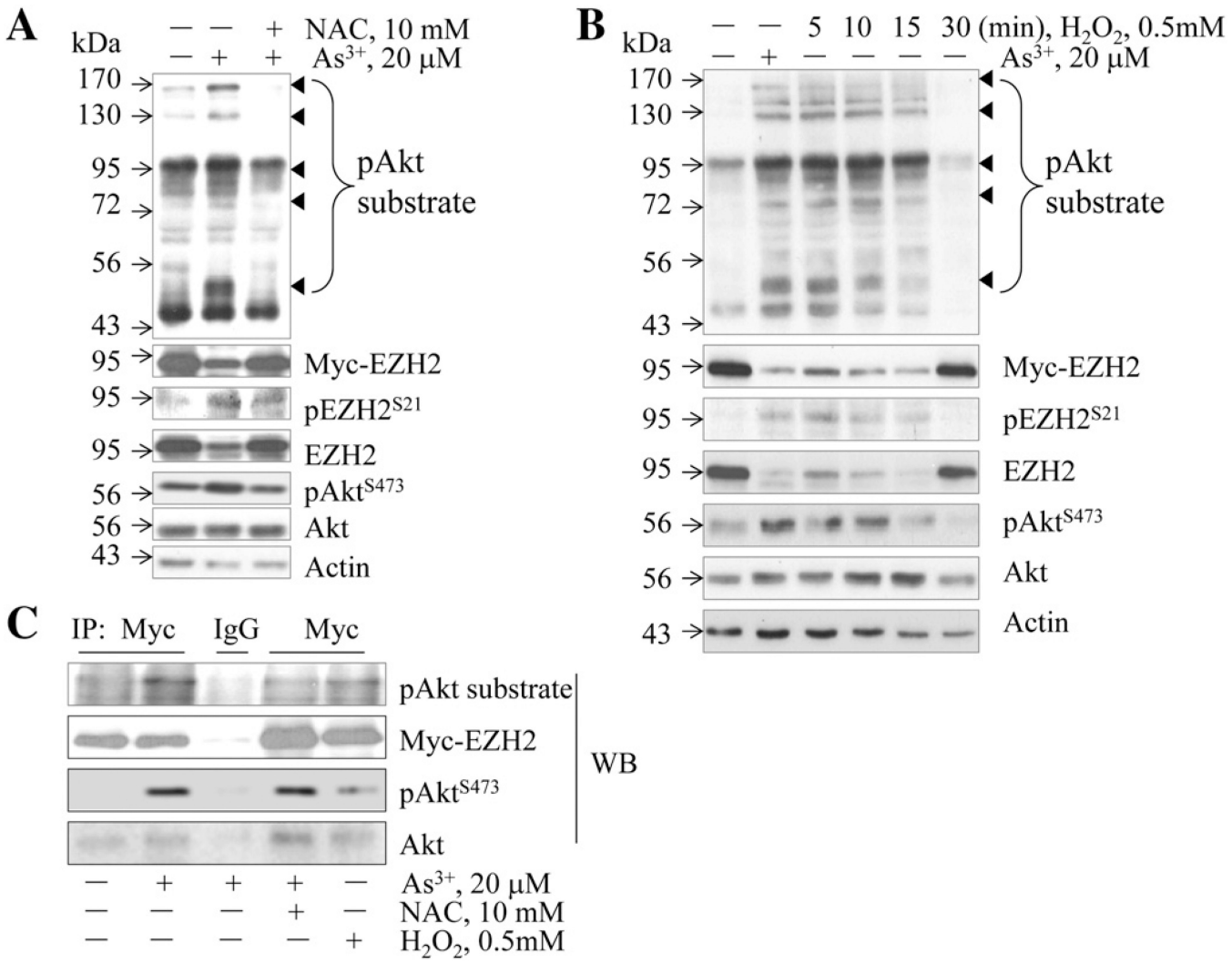

Fig. 3.

Both As^{3+} and H_2O_2 induce the interaction of Akt and EZH2 and Akt-dependent phosphorylation of the exogenous EZH2 overexpressed in HEK-293 cells. (A) HEK-293 cells were transfected with 3myc-tagged EZH2 expression vector for 24 h followed by the treatment of the cells with 20 μM As^{3+} for 2 h in the presence or absence of 10 mM NAC, followed by Western blotting using the indicated antibodies. (B) The transfected HEK-293 cells were treated with As^{3+} or H_2O_2, followed by Western blotting as in (A). (C) Anti-myc tag or control IgG was used in immunoprecipitation (IP) to pull down the exogenousmyc-tagged EZH2. The IP was then subjected to Western blotting using antibodies recognizing the phosphorylated Akt substrate motif (RXRXXS*/T*), myc tag, pAkt, and Akt.

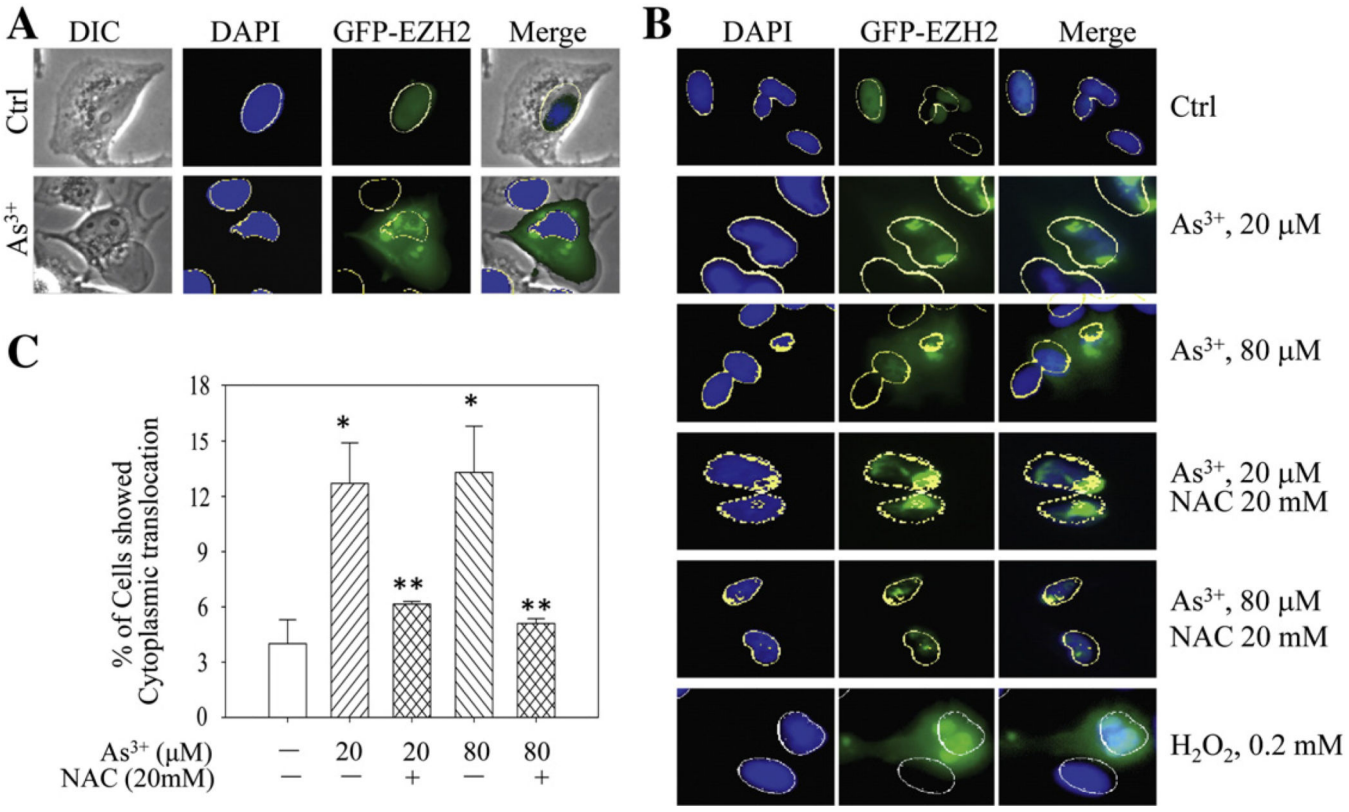

Fig. 4.

Both As^{3+} and H_2O_2 induce cytoplasmic localization of the EZH2 protein in BEAS-2B cells. (A) BEAS-2B cells expressing GFP-EZH2 were treated with 20 μM As^{3+} for 2 h. The intracellular distribution of EZH2 was determined by immunofluorescent microscopy. (B) NAC prevented cytoplasmic localization of the EZH2 protein induced by As^{3+} in BEAS-2B cells transfected with GFP-EZH2. H_2O_2 was used as a control of ROS. (C) Statistical analysis of the cytoplasmic translocation ratio of the EZH2 protein in the cells treated with As^{3+} in the presence or absence of NAC. Data are expressed as the mean ± SD, n=3, ** p < 0.05.

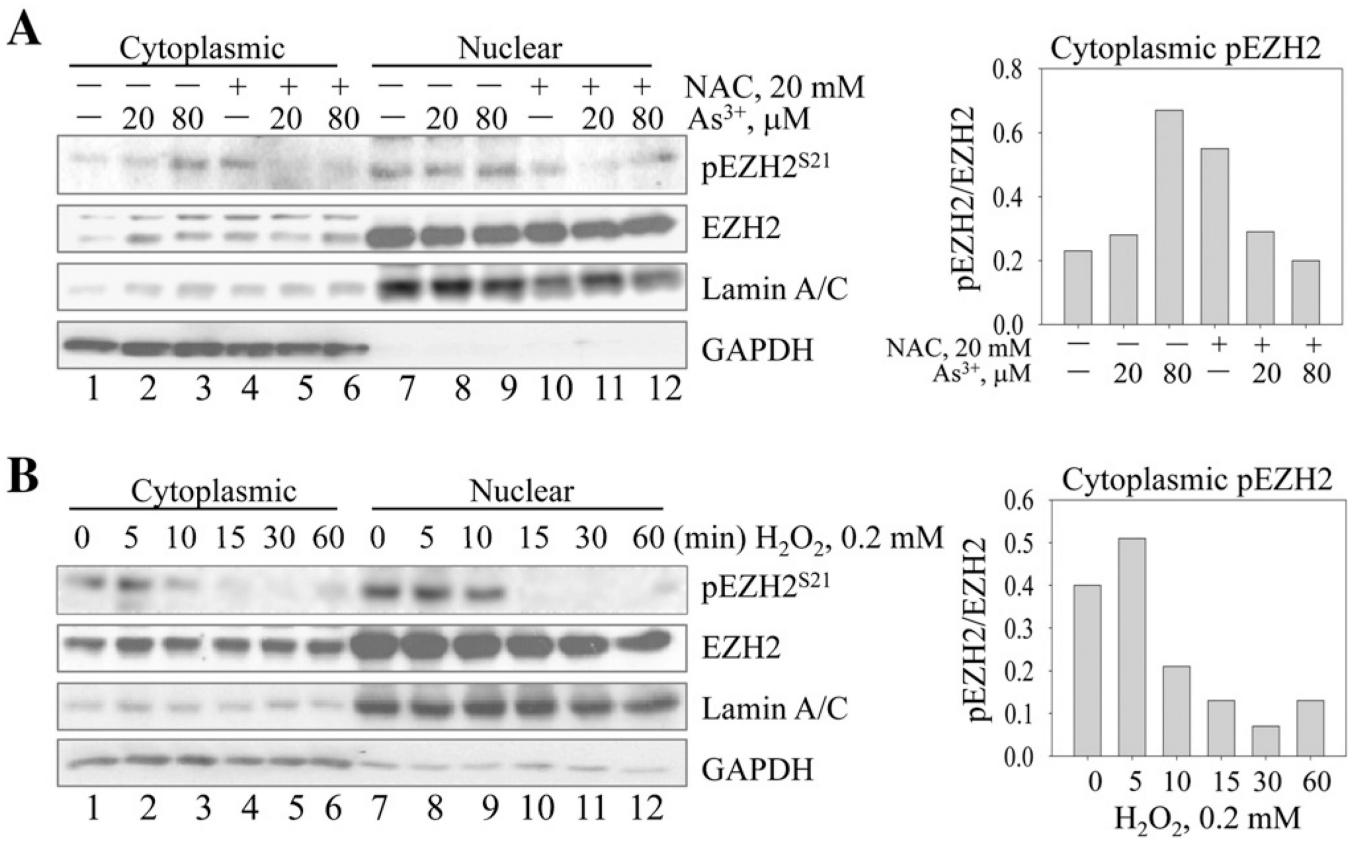

Fig. 5.

Increased cytoplasmic localization of the phosphorylated and total EZH2 in BEAS-2B cells treated with As^{3+} or H_2O_2. (A) BEAS-2B cells were treated with 20 or 80 μM As^{3+} for 2 h with or without NAC pretreatment. Cellular fractions were made to extract the cytoplasmic and nuclear proteins. Lamin A/C and GAPDH were used as indications of the nuclear and cytoplasmic fractions. Lanes 4 and 10 are NAC only groups. Right panel shows semi-quantification of the ratio between pEZH and EZH2 in the cytoplasm. (B) BEAS-2B cells were treated with 0.2 mM H_2O_2 for the indicated times. The levels of phosphorylated EZH2, total EZH2, lamin A/C, and GAPDH were determined in the cytoplasmic and nuclear fractions, respectively. Right panel shows semi-quantification of the ratio between pEZH and EZH2 in the cytoplasm.